The effects of flow rate variation and vegetation ageing on the longitudinal mixing and Residence Time Distribution (RTD) in a full-scale constructed wetland

Vasiliki G. Ioannidou[1], Jonathan M. Pearson[1]

[1] School of Engineering, University of Warwick, Coventry, CV4 7AL, UK

(V.Ioannidou@warwick.ac.uk; J.M.Pearson@warwick.ac.uk)

ABSTRACT

A field-based experimental study has been undertaken within a full-scale constructed wetland, designed to treat runoff from agricultural land in Knapwell, Cambridgeshire, UK. The effects of flow rate variation and natural vegetation ageing on the mixing characteristics are investigated over a eight month period. Detailed fluorometric measurements were made to examine the longitudinal spreading of a solute within the wetland. Between a UK November winter period, and June summer period, 125 tracer tests were undertaken for a range of dry weather and storm flow conditions, using an automated daily injection tracer system. The longitudinal dispersion results show that the dispersion is influenced by the flow rate for low discharge conditions, however, for higher discharges, the longitudinal dispersion becomes independent of discharge. Residence Time Distribution (RTD) curves are examined through a series of flow conditions for each testing month, ranging from transitional (Re~2000) to turbulent (Re~7000) flow conditions. For the conditions measured, differing flow rates produce changes in the RTD, demonstrating that higher flow rates induce shorter mean residence times, generating predominantly an advective flow regime. The effects of plant age are prominent on the mixing pattern. Towards the end of the plant annual cycle, in February/March, mixing pattern approaches complete mixing, longitudinal mixing increases significantly due to long tails on the RTDs, and mean flow velocity is retarded. This indicates that the dormant plant

period, which normally takes 5-6 months (October to March), alters progressively the mixing pattern in the system in such a way that it is significantly different from the mixing pattern during the growing plant season.

RESEARCH HIGHLIGHTS

- Repeatable tracer tests conducted over 8 months on a full-scale constructed wetland
- Testing period covers the total dormant plant season and the new plant growth season
- Reduction peak concentration by up to 3 times may be achieved in late dormant season
- Stronger affinity of HRT, mixing and flow structure with plant season than discharge
- Longitudinal dispersion coefficient increases with flow rate
- Longitudinal dispersion coefficient is vegetation dominated for lower discharges
- Longitudinal dispersion coefficient varies with plant stage

ABBREVIATIONS

CW, constructed wetland; HRT, hydraulic residence time; FWS, free-water surface; RTD, Residence Time Distribution; CRTD, Cumulative Residence Time Distribution; CSTR, continuous stirred tank reactor; TIS, tank in series, RWT, Rhodamine WT.

Keywords: free-water surface constructed wetlands; longitudinal mixing; vegetation ageing; agricultural runoff; flow rate variation; residence time distribution curves; decay plant period

1. INTRODUCTION

Interplay between water and vegetation governs the wetland treatment processes (including physical, chemical and biological). Water movement plays key role in the removal of pollutants, as it identifies the hydraulic residence time (contact and activity time) for treating the pollutants (Jadhav & Buchberger, 1995; Kadlec, 1994; Min & Wise, 2009; Werner & Kadlec, 2000; Jenkins & Greenway, 2005). Vegetation has also a prominent effect on the wetland hydrodynamics and performance, because it generates flow resistance; changes the velocity field and hence turbulence levels, and affects the mixing characteristics (Jadhav & Buchberger, 1995; Kadlec, 1990; Jenkins & Greenway, 2005; Nepf, 2012a). Nepf (2012) reported that uncertainty exists between the seasonal variation of vegetation characteristics and discharge. Furthermore, plant growth cycle (including the growing and decay periods), and plant ageing can affect the residence time and the mixing characteristics/regime in the system. Heterogeneities in morphology and vegetation porosity, and the plant patches and wetland boundaries might enhance mixing through greater turbulence levels (Ghisalberti and Nepf, 2005; Okamoto et al., 2012). Various types of constructed wetlands (CWs) are currently in use to mitigate or remove a wide variety of contaminants. Particularly though, free-water surface (FWS) wetlands with emergent vegetation have demonstrated higher efficiency on nutrients removal (Kadlec, 2009; Weisner & Thiere, 2010); nevertheless, there is still a paucity of scientific data evaluating the performance of full-scale CWs.

To-date, the majority of experimental studies relevant to investigation and optimization of CWs hydraulic performance factors (aspect ratio, inlet/outlet configuration, obstruction designation), have overlooked both the role of vegetation on the hydraulic performance or/and have been largely applied in ideal systems' shapes (Persson, 2000; German et al, 2005; Su et al, 2009; Aguwamba, 2006). The impact of vegetation on transport processes has been studied by Kadlec, 1990, Nepf et al, 1997, Nepf, 1999, Wörman & Kronnäs, 2005, Nepf et al, 2007, Burke & Wadzuk, 2009, Sabokrouhiyeh et al, 2017. However, the majority of the existing experimental studies have been applied using artificial vegetation on pilot scale units (Nepf et al, 1997; Chyan et al, 2014), while there are few studies that have examined natural vegetation either in laboratory conditions (Shucksmith, 2008) or in full-scale aquatic environments (Lightbody & Nepf, 2006). In addition, the number of tracer tests undertaken in most studies is limited, and refers to a short time period (either single/same day or week), which omits the seasonal change of vegetation (growth or decay stages), and its possible effects on transport processes (mixing), and on residence time (Somes et al, 1998; Koskiaho, 2003; Nepf, 1999; Lightbody & Nepf, 2006; Nepf et al, 2007; Kröger et al, 2009; Nepf, 2012a; Nepf, 2012b; Chyan et al, 2014).

This paper presents results from a full-scale field CW implementing repeatable/multiple tracer tests, and covering an eight-month monitoring period. The main aim of the paper is to determine the effects of plant ageing (especially during the decay plant period) on the hydraulic residence time (HRT), and the mixing characteristics of a FWS constructed wetland with fully emergent vegetation, and to provide empirical data. Tracer tests were undertaken on a daily basis (from the end of a UK autumn until the start of summer), using an automated tracer injection and data collection system. This allowed the investigation of different flow rates on the mixing characteristics and HRT, to be determined.

2. MATERIAL & METHODS

2.1 Site description & experimental setup

The experimental test programme was conducted on a FWS CW designed to treat runoff from agricultural land in Knapwell, Cambridgeshire, UK. The system is of irregular shape (Figure 1) and has average length 35 m and average width 10 m. The water depth varies depending on the flow rate (as a result of water drained from drainage system due to precipitation), but did not deviate more than 0.2 m in the main body of the wetland, for the flow conditions tested. The flow in the CW is dependent on the seasonal precipitation pattern, and discharges through the surrounding fields drainage system. The wetland is unbunded (non-walled) at the outlet, and constitutes a shallow, flow-through system. Normally, continuous flow is maintained through base flow between October and March, while during the summer months, the phreatic layer drops, resulting in intermittent flow periods occurring from surface water runoff, following a period of precipitation. The rainfall – runoff record for the monitoring period November 2015 to June 2016 is shown in Figure 2. The CW plan map is illustrated in Figure 1, indicating the shape and depth of the wetland (with contour lines spacing every 0.2 m), the hydraulic control structures, the dye injection location by the arrow indicator, the approximate maximum plan surface area of the water banks for the highest flow rate conditions tested (indicated by the inner black continuous line), the vegetation area (indicated by plus symbol as undertaken in the main June 2014 survey), and the internal mixing study locations (indicated by stars). The bed slope from the inlet to outlet is 0.007 (0.7%). There are calibrated hydraulic control structures at the inlet and outlet to monitor the flow rate. An instrumented V-notch weir is installed at the inlet, and a Venturi flume at the outlet. The dye injection point is 2 m downstream of the V-notch weir. A secondary check on the flow is measured through dilution gauging.

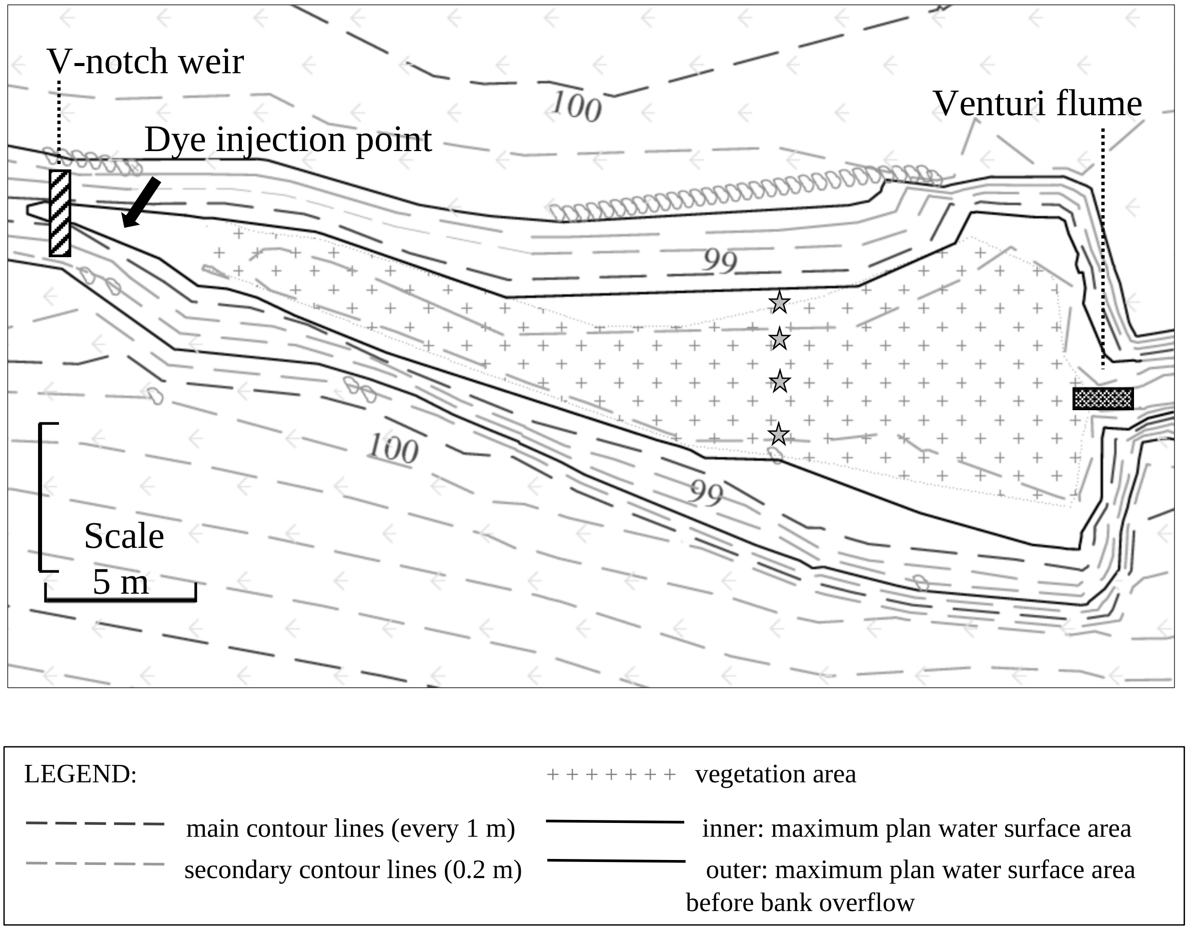

Figure 1: Constructed Wetland plan topographic map. The map indicates the hydraulic control structures at the inlet and outlet, the dye injection point, and the four internal mixing measuring locations (by star) on the particular cross-section, approximate maximum plan surface area of water banks for highest discharge conditions tested, vegetation area (by plus symbol).

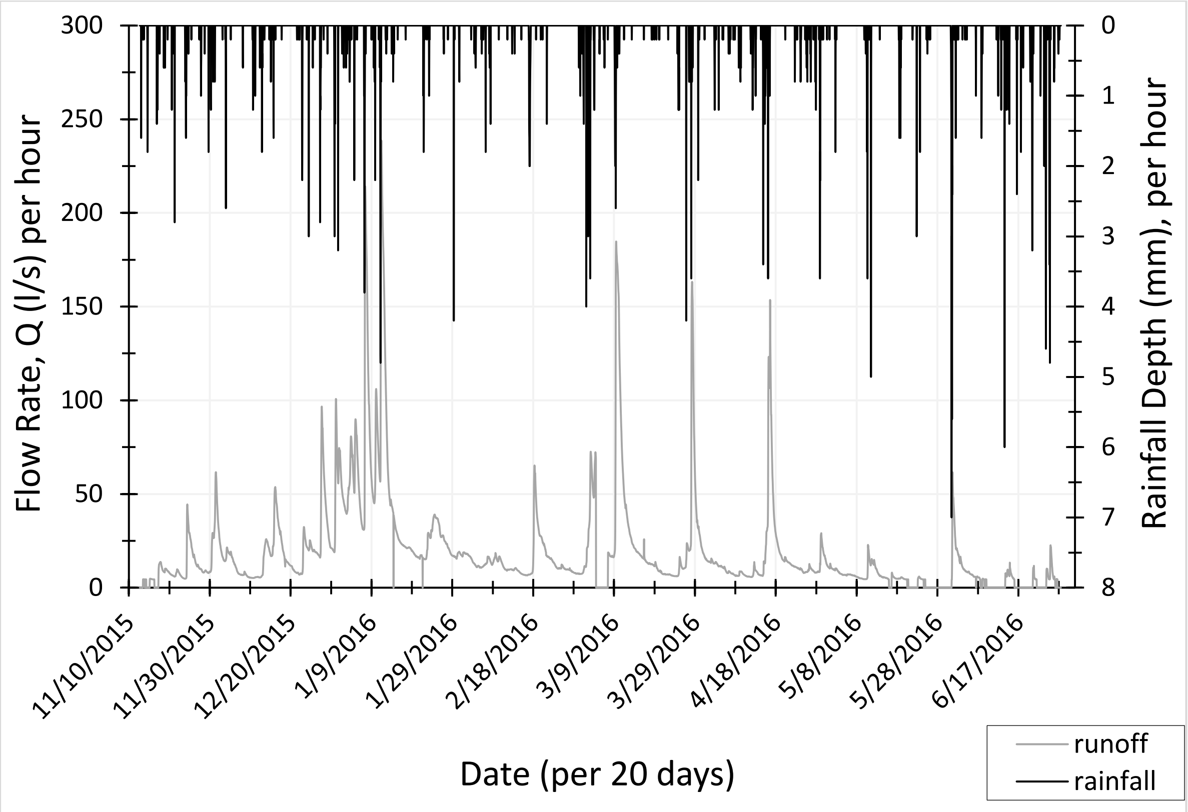

Figure 2: Rainfall – Runoff plot during the monitoring period November 2015 – June 2016.

No irrigation scheme is applied to the surrounding fields, thus the flow rate variation is both a function of rain intensity, duration, and percentage runoff. Consequently, the CW volume is a function of the precipitation and season. Vegetation is fully emergent and monoculture, vegetated by Phragmites australis. Plant cycle is annual and is distinguished between spring-summer (plant growth period, when new macrophytes grow and evolve), and autumn-winter cycle (plant decay period; plant growth ceases and wither occurs until the end of annual cycle). In this micro-climate, stems develop and grow up from April to September, and they wither and decay progressively from October until the end of March, entailing lower resistance and flexibility against the flowing water, as well as higher stem deflection. Typical vegetation conditions between contrasting seasons are illustrated in Figure 3.

2.2 Seasonal Vegetation characteristics

Phragmites stem diameters have been monitored between November 2015 and July 2016, where selected stems were marked, and the same stems were monitored every one or two months for their diameter variation. A record of the stem diameters and number of measurements is shown in Table 2.1. In June the plants are approximately 1.5-2.0 m in height (see Figure 3, Left), still developing until approximately September. Between September and October the plant growing (or developing) season ceases, and plants enter the dormant season (October to March). During the dormant season (October to March), when at least half of the present tests were conducted (see Figure 3, Right), the stems morphology alters; their foliage falls and they tend to bend over or break, creating clusters, while their resistance reduces. Stem resistance is maximum at the maturity of the plant growth cycle (Shih & Rahi, 1982). During the new developing season, commencing in April, some half-broken, old decayed stems remain in upright position, and are intermingled with the new generation. The mean diameter of the new and old cycle stems is indicatively for June d_{June_New}= 5.80 mm and d_{June_Old}= 5.34mm respectively.

Figure 3: (Left) Picture showing the developing plant stage, June, with flourishing stems. (Right) Picture taken from the outlet showing the winter dormant stage, December.

Table 2.1: Stem diameters.

Plant Cycle	Name of stem	Number of stem measurements	Mean stem diameter, d (mm)	Standard deviation	Standard error	Mean stem density, n (n/m^2)
OLD (2014-2015)	SW1_C	4	6.58	0.31	0.22	208
	SW1_D	5	5.95	0.25	0.18	
NEW (2015-2016)	NG_SW1_C	4	5.38	0.21	0.15	174
	NG_SW1_D	4	5.29	0.16	0.12	

Where d = stem diameter (mm), and n = number of stems per unit area (that is per m^2).

To measure the vegetation porosity, η, the stem diameter, d, of Phragmites was assumed to be constant with depth, as the cylindrical nature of stems allow this approximation. In this way, the plant porosity was calculated as $\eta = 1 - \Phi$. This equation is characterised by the stem population density, n, per unit area (namely m^2), and the plant solid volume fraction, Φ $(= n\pi d^2/4)$. For the growth (developing) plant period, the calculated vegetation porosity is η_g = 0.995, where g stands for growing. This indicates that only 0.5% of vegetation, that is live and upright, accounts for the wetland volume, a value that plays negligible role in the calculation of the wetland volume, and infers that stems density is sparse. The CW volume ranges between 34 and 75 m^3 for the tested conditions of this study. Porosity of the fully deflected scenario during the dormant season was difficult to calculate. Approximation of the vegetation porosity for the dormant period was attempted, giving η_d = 0.959, where d stands for decay, albeit such value is only indicative. This porosity was approximated applying the worst case scenario, in which the plants are assumed to be fully-deflected, and submerged in the wetland, refering to February and March (end of plant cycle). In this case, the difference between no plants ($\eta_0=1$) and fully deflected plants accounts for 8.2% of the CW volume, which implies that plants occupy only a small fraction of the wetland volume. Under this assumption, the volume during February-March is calculated to range between 31 – 69 m^3 for the flow rates presented in this study.

2.3. Tracer tests & Longitudinal Mixing

Field hydraulic tracer experiments were carried out in autumn – winter – spring months in 2015–2016. The site proximity and seasonal flow nature brought the need of an in-situ automated tracer injection system, which was developed and deployed for the testing period. The tracer used in this study was Rhodamine WT (RWT) fluorescent dye, since it is a conservative fluorescence tracer, and easily detectable at low concentrations (less than 0.1 part per billion).

Slug tracer injections were employed to obtain the longitudinal mixing, discharge (through dilution gauging) and Residence Time Distributions (RTD). The tracer concentrations were measured at the outlet of the CW, using submersible fluorometers Cyclops-7 (Turner Designs) with a continuous 1 Hz logging rate, and using Novus LogBox data banks (averaged over 60 s). For the testing period, the water level was recorded at the inlet v-notch weir to determine the discharge, and a micro-controller was programmed to inject the tracer at specific time intervals. The subsequent spreading of the tracer was recorded continuously for a certain amount of hours (based on the season and discharge levels), following the pulse injection.

Over the experimental testing period, 125 tests were carried out at a range of discharges (between 0.4 and 68.2 l/s). Established techniques to undertake pre-processing data analysis, instrument calibration, background concentration removal, identification of start/end points of each tracer distribution curve (when the measured concentration falls below 1.0% of the peak value for more than 30 s), were adopted. Employing the concept of Taylor (1953), the longitudinal dispersion coefficient (D_x), was determined using Equation 1:

$$D_x = \frac{u^2}{2}\frac{d\sigma_t^2(x)}{dt} \qquad \text{Equation 1}$$

where u = velocity in the longitudinal direction (m/s), σ^2 = variance (s^2) , x = distance downstream (m), and t = time (s)

2.4 Fluid & Flow properties & Flow Measurement

The primary method to measure the flow rate was through a pressure transducer installed on the V-notch weir. The water level was converted to flow rate through standard calibration algorithms (BS 3680-4A: 1981). As a secondary check, dilution gauging (BS 3680-2A; 1995) was used to verify flow rates by Equation 2;

$$Q = \frac{VC_1}{\int_{t1}^{t2}(C_2 - C_0)dt} \qquad \text{Equation 2}$$

where C_1= injected tracer concentration (ppb); C_0 = background tracer concentration (ppb); C_2 = downstream measured concentration (ppb); V = volume of tracer introduced (m^3); t = time (s).

In Newtonian fluids, like water, kinematic viscosity, v, varies with temperature. The water temperature was logged, and a mean water temperature for reach month was calculated. Based on that, there were selected two mean v values, as v_{winter} =$1.446 \cdot 10^{-6}$ m^2/s, referring to winter months (November to March), and v_{summer} =1.167·10-6 m^2/s, referring to summer season (April to October). Flow classification is determined by the Reynolds number, Re, defined as in Equation 3:

$$\mathrm{Re} = u \cdot h/\nu \qquad \text{Equation 3}$$

where u = flow velocity (m/s) and h = water depth in open channel flow (m).

2.5 Residence Time Distribution (RTD) data analysis

In plug flow theory, where all water parcels are assumed to traverse the wetland at the same velocity and exit at the same time, it is customary to adopt the theoretical or nominal residence time, t_n. This is denoted as the fraction of the wetland volume over the flow rate. However, this basic standard rule might not fit well in actual wetland conditions, due to: variations in flow velocity, heterogeneous mixing processes (mainly due to bed topography and spatial vegetation distribution), and wind interference, all of which create a distribution of residence times in each water particle entering the system, ultimately leading to a distribution of travel times. These deviations from the ideal pattern cause some water particles to depart earlier or later from the system resulting either in short-circuiting or low velocity zones (Thackston et al, 1987). The RTD function *E(t)* is defined as Equation 4:

$$E(t) = \frac{Q(t)C(t)}{\int_0^\infty Q(t)C(t)dt} \cong \frac{Q(t)C(t)}{\sum_{i=1}^{n} Q(t)C(t)dt} \qquad \text{Equation 4}$$

where $E(t)$ = RTD function (s^{-1}); $Q(t)$ = outlet flow rate at time t ($m^3\ s^{-1}$); $C(t)$= outlet tracer concentration at time t (ppb); t = sampling time (s); dt = sampling time interval (s).

The mean residence time, t_m, is the average time that a tracer particle has stayed in the wetland. It is defined as the first moment of the RTD (also known as the centroid), given by Equation *5*:

$$t_m = \int_0^\infty tE(t)dt \cong \sum_{i=1}^{n} tE(t)dt \qquad \text{Equation 5}$$

Variance, σ^2 (s^2), is a measure of the RTD spread and corresponds to the second moment, computed by Equation 6:

$$\sigma^2 = \int_0^\infty (t_m - t)^2 E(t)dt \cong \sum_{i=1}^{n} (t_m - t)^2 E(t)dt \qquad \text{Equation 6}$$

while dimensionless variance is calculated as the fraction of variance over the square of the mean residence time, given by Equation 7:

$$\sigma_\theta^2 = \frac{\sigma^2}{t_m^2} \qquad \text{Equation 7}$$

The tank in series (TIS) model has shown good capability in describing non-ideal flow (Kadlec & Wallace, 2009) processes. As such, the wetland is divided into an equal number of completely stirred tank reactors (CSTR) represented by Equation 8:

$$N = \frac{t_m^2}{\sigma^2} \qquad \text{Equation 8}$$

in which t_m = mean residence time of the RTD, and σ^2 = variance of the RTD.

The hydraulic efficiency, λ, enables a comparison between different systems. The λ parameter is a measure of the CW capacity to distribute the flow equably within the occupying water volume, and also to attain adequate mixing or recirculation (Persson et al, 1999). Consequently, the plug flow pattern does not seem an appropriate modelling approach for vegetated systems, as some degree of mixing is essential to spread the pollutant around/across, and to achieve reduction of the pollutant peak concentration. Persson et al (1999) have classified the hydraulic efficiency into bands, as listed in Table 2.2. The hydraulic efficiency in this paper was calculated as in Equation 9 (Bodin et al, 2012; Chyan et al, 2014):

$$\lambda = \frac{t_p}{t_m} \qquad \text{Equation 9}$$

in which t_p = peak concentration time (s) of the RTD.

Table 2.2: Hydraulic efficiency classification (Persson et al, 1999).

Quality of λ	Range factor
Good	$\lambda>0.75$
Satisfactory	$0.5<\lambda\leq0.75$
Poor	$\lambda\leq0.5$

The shortest travel time, t_1', from the inlet to the outlet identifies short-circuiting. This refers to the quickest flow path in the system and corresponds to the first arrival time of the tracer at the outlet. This is the minimum travel time from the inlet to the outlet. The short-circuiting index in this study was defined as the fraction of t_1' over the mean residence time, t_m, given in Equation 10:

$$S_m = \frac{t_1'}{t_m} \qquad \text{Equation 10}$$

3. RESULTS & DISCUSSION

Over a period of eight months, 125 tracer tests were carried out. A summary of the complete test series is shown in Table 3.1, providing details of several RTD analysis parameters. The unique test code column defines the flow rate regime as low (L), moderate (M), high (H), and extreme (E), followed by the number of the month (from 01 for January to 12 for December) that the tracer took place, and the test number in ascending order for that particular month. The flow rate ranged between 0.4 and 68.2 l/s.

Table 3.1: Summary of test series & transport parameters from the RTD analysis 125 tests.

Test unique code	*Month*	*Flow Rate regime*	*Flow rate, Q* (l/s)	*First arrival time, t_1'* (min)	*Travel time, t_m* (min)	*Nominal residence time, t_n* (min)	*Longitudinal Dispersion coefficient, D_x* (m^2/s)	*Number of CSTR, N*	*Hydraulic efficiency λ (t_p/t_m)*	*Effective volume ratio, e (t_m/t_n)*
L,11,1	Nov		3.4	9.8	20.1	45.5	0.211	2	0.7	0.4
L,11,2	Nov		2.4	13.5	29.8	55.6	0.063	5	0.7	0.5
L,11,3	Nov		4.7	10.0	17.5	37.5	0.054	10	0.8	0.5
L,12,1	Dec		3.7	12.5	21.5	43.6	0.029	14	0.9	0.5
L,12,2	Dec	Low	2.8	13.5	25.8	51.1	0.059	6	0.8	0.5
L,12,3	Dec		2.9	12.5	24.5	51.1	0.056	7	0.8	0.5
L,12,4	Dec		3.0	12.5	23.4	48.9	0.052	7	0.8	0.5
L,02,1	Feb		5.0	11.0	34.9	36.3	0.109	2	0.5	1.0
L,03,1	Mar		3.9	12.5	31.3	42.1	0.105	3	0.7	0.7

L,03,2	Mar		2.9	11.0	41.4	51.1	0.267	1	0.5	0.8
L,03,3	Mar		2.6	12.0	34.9	53.3	0.147	2	0.7	0.7
L,03,4	Mar		2.2	13.0	35.5	59.1	0.070	4	0.7	0.6
L,03,5	Mar		2.0	13.0	34.7	62.5	0.047	6	0.8	0.6
L,03,6	Mar		1.8	13.5	32.6	66.0	0.027	10	0.8	0.5
L,03,7	Mar		1.8	13.5	42.3	67.8	0.129	2	0.6	0.6
L,04,1	Apr		3.5	7.5	24.3	62.3	0.078	5	0.7	0.4
L,04,2	Apr		4.4	9.5	21.4	51.6	0.082	5	0.7	0.4
L,04,3	Apr		1.9	13.5	30.9	64.3	0.039	8	0.8	0.5
L,04,4	Apr		4.2	11.0	20.7	39.8	0.052	8	0.8	0.5
L,04,5	Apr		2.0	12.5	26.8	62.5	0.047	7	0.8	0.4
L,04,6	Apr		4.1	11.0	24.8	41.3	0.093	4	0.7	0.6
L,05,1	May		3.4	13.5	33.2	45.5	0.043	6	0.8	0.7
L,05,2	May		2.7	16.0	53.9	55.6	0.084	2	0.4	1.0
L,05,3	May		0.6	19.0	45.9	144.6	0.061	3	0.6	0.3
L,05,4	May		3.5	12.5	22.2	45.5	0.042	10	0.8	0.5
L,05,5	May		0.4	15.0	38.1	156.6	0.040	6	0.7	0.2
L,05,6	May		0.6	22.0	53.5	150.6	0.032	5	0.8	0.4
L,06,1	June		4.2	8.5	15.4	40.5	0.091	6	0.8	0.4
L,06,2	June		2.4	9.5	17.3	55.6	0.042	12	0.8	0.3
L,06,3	June		1.2	10.5	20.9	90.9	0.043	10	0.8	0.2
L,06,4	June		4.4	8.0	13.9	50.0	0.065	10	0.8	0.3
M,11,1	Nov	Moderate	5.9	9.3	18.5	33.7	0.200	2.5	0.7	0.5
M,11,2	Nov		6.8	9.0	17.2	31.7	0.187	2.8	0.7	0.5
M,11,3	Nov		8.9	8.7	17.0	28.4	0.208	2.6	0.7	0.6
M,11,4	Nov		7.8	7.8	17.4	30.0	0.391	1.3	0.6	0.6
M,11,5	Nov		8.2	8.5	18.5	29.3	0.300	1.6	0.6	0.6
M,11,6	Nov		7.7	9.0	15.7	30.0	0.096	6.0	0.8	0.5
M,11,7	Nov		8.0	8.8	14.4	29.7	0.068	9.2	0.8	0.5
M,12,1	Dec		9.0	9.0	14.4	28.2	0.065	9.7	0.9	0.5
M,12,2	Dec		8.0	9.5	15.8	29.7	0.080	7.2	0.8	0.5
M,12,3	Dec		7.3	9.5	16.1	30.7	0.074	7.6	0.8	0.5
M,12,4	Dec		6.6	10.0	16.7	32.0	0.078	7.0	0.8	0.5
M,02,1	Feb		6.6	9.5	24.2	32.0	0.163	2.3	0.6	0.8
M,02,2	Feb		7.5	7.5	23.1	30.7	0.152	2.6	0.6	0.8
M,02,3	Feb		6.6	9.0	23.6	32.0	0.180	2.1	0.6	0.7
M,02,4	Feb		8.0	8.5	19.9	29.7	0.164	2.8	0.7	0.7
M,02,5	Feb		8.5	8.5	19.4	29.0	0.154	3.0	0.7	0.7
M,02,6	Feb		5.3	11.0	32.3	35.4	0.110	2.6	0.5	0.9
M,02,7	Feb		5.5	10.5	31.7	35.0	0.109	2.6	0.5	0.9
M,02,8	Feb		5.6	11.0	37.3	34.5	0.091	2.7	0.5	1.1
M,02,9	Feb		8.0	9.5	19.1	29.7	0.101	4.7	0.7	0.6
M,02,1	Feb		8.1	9.0	21.4	29.3	0.140	3.0	0.7	0.7
M,02,1	Feb		6.8	10.0	23.9	31.7	0.129	2.9	0.6	0.8
M,02,1	Feb		5.4	11.5	35.2	35.4	0.167	1.5	0.5	1.0
M,02,1	Feb		5.5	9.5	34.0	35.0	0.113	2.4	0.6	1.0
M,03,1	Mar		5.3	10.0	25.5	35.4	0.108	3.3	0.7	0.7
M,03,2	Mar		8.2	8.0	18.6	29.0	0.123	3.9	0.8	0.6
M,03,3	Mar		7.3	8.5	22.6	30.7	0.212	1.9	0.7	0.7
M,03,4	Mar		8.7	7.5	14.8	30.1	0.052	11.9	0.9	0.5
M,03,5	Mar		6.2	8.5	21.0	38.9	0.174	2.5	0.8	0.5
M,03,6	Mar		5.8	9.0	23.7	41.0	0.334	1.1	0.7	0.6
M,04,1	Apr		8.6	6.5	15.9	30.4	0.313	1.8	0.7	0.5
M,04,2	Apr		8.3	7.5	13.9	31.1	0.088	7.4	0.8	0.4
M,04,3	Apr		7.0	7.5	13.7	35.4	0.080	8.3	0.8	0.4
M,04,4	Apr		6.8	8.5	18.4	36.4	0.121	4.1	0.7	0.5
M,04,5	Apr		6.0	8.5	18.2	39.9	0.119	4.2	0.7	0.5
M,04,6	Apr		5.5	9.0	18.4	42.9	0.066	7.5	0.7	0.4
M,04,7	Apr		8.2	8.0	15.8	29.3	0.156	3.7	0.8	0.5
M,04,8	Apr		6.9	8.5	17.3	31.7	0.118	4.4	0.8	0.5
M,06,1	June		9.0	6.5	11.3	28.2	0.155	5.2	0.8	0.4
M,06,2	June		5.5	7.5	12.8	35.0	0.098	7.3	0.8	0.4
H,11,1	Nov	High	10.5	8.0	13.3	26.3	0.092	7.4	0.8	0.5
H,11,2	Nov		9.4	8.3	15.9	27.6	0.241	2.4	0.7	0.6

H,11,3	Nov		11.0	7.2	14.5	25.8	0.378	1.7	0.7	0.6
H,12,1	Dec		10.5	8.0	13.2	26.3	0.059	11.5	0.9	0.5
H,12,2	Dec		9.7	8.5	14.2	27.3	0.071	9.0	0.8	0.5
H,12,3	Dec		9.1	10.5	16.9	27.9	0.036	15.0	0.9	0.6
H,02,1	Feb		11.9	7.5	15.2	24.9	0.151	4.0	0.8	0.6
H,02,2	Feb		10.2	8.0	17.6	26.5	0.198	2.6	0.7	0.7
H,02,3	Feb		11.0	7.5	16.8	25.8	0.222	2.4	0.7	0.7
H,02,4	Feb		14.1	7.0	15.4	23.3	0.206	2.9	0.7	0.7
H,02,5	Feb		10.0	8.0	18.7	27.1	0.151	3.2	0.6	0.7
H,02,6	Feb		10.4	8.0	20.5	26.5	0.180	2.5	0.6	0.8
H,02,7	Feb		12.7	8.0	19.3	24.3	0.211	2.2	0.6	0.8
H,02,8	Feb		9.3	9.0	17.4	27.9	0.065	8.0	0.8	0.6
H,03,1	Mar		13.9	8.5	15.9	23.3	0.142	4.0	0.8	0.7
H,03,2	Mar		12.9	6.5	18.8	24.0	0.429	1.1	0.5	0.8
H,03,3	Mar		11.3	7.0	17.6	25.4	0.277	1.9	0.7	0.7
H,03,4	Mar		13.6	6.0	10.0	21.7	0.111	8.1	0.8	0.5
H,03,5	Mar		11.9	6.0	10.8	23.9	0.117	7.2	0.8	0.5
H,03,6	Mar		10.7	6.5	11.1	25.8	0.092	8.8	0.9	0.4
H,04,1	Apr		9.7	6.5	11.6	27.8	0.085	9.2	0.8	0.4
H,04,2	Apr		10.8	6.5	12.2	25.5	0.136	5.5	0.8	0.5
H,04,3	Apr		9.1	6.5	12.9	29.1	0.157	4.5	0.8	0.4
H,04,4	Apr		9.4	7.0	14.3	28.4	0.148	4.3	0.7	0.5
H,04,5	Apr		10.0	7.0	13.2	27.1	0.087	7.9	0.8	0.5
E,11,1	Nov		23.6	6.3	12.0	18.9	0.366	2.1	0.7	0.6
E,11,2	Nov		17.7	6.3	12.7	21.2	0.430	1.7	0.7	0.6
E,12,1	Dec		20.4	7.0	11.7	20.1	0.073	10.6	0.9	0.6
E,12,2	Dec		17.5	7.5	12.6	21.4	0.063	11.3	0.8	0.6
E,12,3	Dec		16.1	7.5	13.1	22.0	0.091	7.7	0.8	0.6
E,12,4	Dec		20.4	7.0	12.1	20.1	0.057	13.1	0.8	0.6
E,12,5	Dec		18.7	7.0	12.7	20.8	0.094	7.6	0.8	0.6
E,12,6	Dec		15.9	7.5	14.0	22.2	0.101	6.4	0.8	0.6
E,02,1	Feb		33.3	5.5	10.8	16.5	0.232	3.6	0.8	0.7
E,02,2	Feb		27.4	5.5	12.3	17.8	0.395	1.9	0.8	0.7
E,02,3	Feb		22.7	6.5	13.6	19.1	0.159	4.2	0.8	0.7
E,02,4	Feb		19.6	6.5	14.9	20.3	0.151	4.0	0.7	0.7
E,02,5	Feb		18.3	7.0	16.4	20.9	0.299	1.8	0.7	0.8
E,02,6	Feb		15.6	7.5	18.4	22.4	0.237	2.1	0.6	0.8
E,03,1	Mar	Extreme	19.6	7.0	12.4	20.3	0.100	7.3	0.8	0.6
E,03,2	Mar		30.4	6.0	10.6	17.0	0.124	6.9	0.8	0.6
E,03,3	Mar		68.2	4.5	8.5	13.7	0.279	3.8	0.8	0.6
E,03,4	Mar		44.6	5.0	9.2	15.2	0.129	7.6	0.9	0.6
E,03,5	Mar		62.1	4.5	8.5	14.0	0.153	7.0	0.9	0.6
E,03,6	Mar		18.5	7.0	13.3	17.4	0.119	5.7	0.8	0.8
E,03,7	Mar		16.1	6.0	12.3	19.2	0.188	3.9	0.7	0.6
E,03,8	Mar		44.9	4.0	7.5	9.8	0.115	10.5	0.9	0.8
E,03,9	Mar		27.7	5.0	8.6	13.3	0.114	9.3	0.8	0.6
E,03,10	Mar		24.1	5.0	8.8	14.5	0.134	7.7	0.9	0.6
E,03,11	Mar		19.1	5.0	11.4	17.0	0.479	1.7	0.7	0.7
E,03,12	Mar		15.7	5.5	9.5	19.5	0.075	12.8	0.8	0.5
E,04,1	Apr		34.2	5.0	7.7	16.3	0.054	22.0	0.9	0.5
E,06,1	June		16.5	5.5	9.0	21.9	0.094	10.7	0.9	0.4
E,06,2	June		17.7	4.0	8.1	21.2	0.343	3.3	0.9	0.4

3.1 Effects of vegetation on velocity profiles & discharge

The effect of vegetation stage on the flow rate and velocity profiles is illustrated in Figure 4**Error! Reference source not found.**, presenting different reeds ages, namely middle (i.e. November), high (i.e. March), and low (i.e. June). The avergage velocity, u_{mean}, is calculated as the ratio of longitudinal distance over time, where the longitudinal distance is fixed (i.e. between injection point and outlet fluorometer point), and time is the HRT (or t_m) obtained through the tracer test. It is observed that the average velocity increases with flow rate in all plant stages, implying production of growing boundary shear with flow rate; however, the rate of the increase varies, depending on the plant stage (or month). Less variation between the channel velocity and the flow rate is noted in February, along with notable flow retardation, particularly attributed to he clusters of deflected stems due to natural ageing, producing lower shear velocity at the bed. At the outset of the new plant cycle, in April, there is greater dependency between the mean velocity and the flow rate, indicating that the bed shear plays a greater role. It is therefore inferred that the upright newly developed stems do not produce enough resistance to the flow, inferring also that their packing density might be rather sparse. According to Nepf et al's (1997) laboratory experiments on wooden dowels population densities, the current stem density, 208 stems m^{-2}, would belong to low population density. Of interest is the disordered nature of March results, which lay between high and low variation between the mean velocity and the discharge. It was observed, that in March – the last month of the plant cycle – the decayed plant material underwent changes and further wither and decomposition, thereby accrediting to this sporadic non-linear trend the larger scatter.

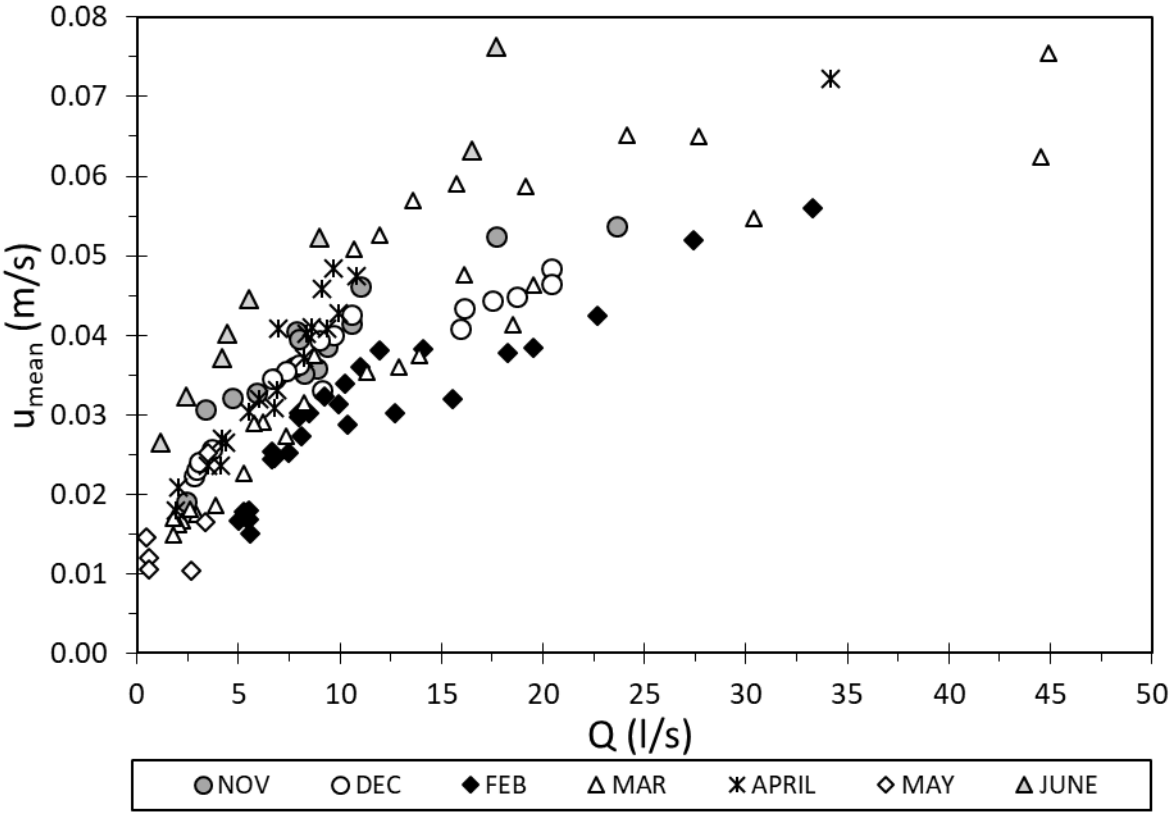

Figure 4: Effects of plant stage on velocity profiles and discharge.

Flow speed accelerates in June (i.e. growth season), finding less resistance because of the upright stems' morphology. Overall, Figure 4 demonstrates that flow velocity is more flow dominated in growth season (i.e. June – November), whilst flow velocity becomes more vegetation dominated at highest ages, as pinpointed by the curved shape obtained in February.

3.2 Effects of seasonal vegetation variation on flow structure and dispersion

As expected, larger flow rate conditions, result in shorter first arrival times, and thus HRTs, of the tracer, as noted from the RTDs in Figure 5. There is a consistent effect of plant season on all flow conditions, where based on the month, the relevant stem morphology (i.e. deflection) and plant friction alter the HRT, the flow pattern and the mixing characteristics.

The seasonal plant variation effects on flow structure for low plant age (i.e. June) exhibit shorter travel times and promote plug flow with minimal longitudinal dispersion, whilst for high plant ages (i.e. February, March) flow retardation and longer distribution tails are observed (see Figure 5). The plant ageing effect is more influential, particularly at the end of the dormant period (coinciding with the end of the annual plant cycle), namely in March. This is because stems progressively decay and tend to bend over, to deflect and to nest in bunches, which alters both the channel porosity, and the internal mixing (by increasing it). Seasonal plant variation also affects the mixing pattern, which combines plug flow and backmixing (dead zones); predominantly in high plant ages (i.e. February and March), flow structure experiences a large quantity of dead regions. This is because beyond November stems decay progressively, and bend over, deflect and nest in clusters, thus altering the channel porosity, flow velocity, and mixing characteristics.

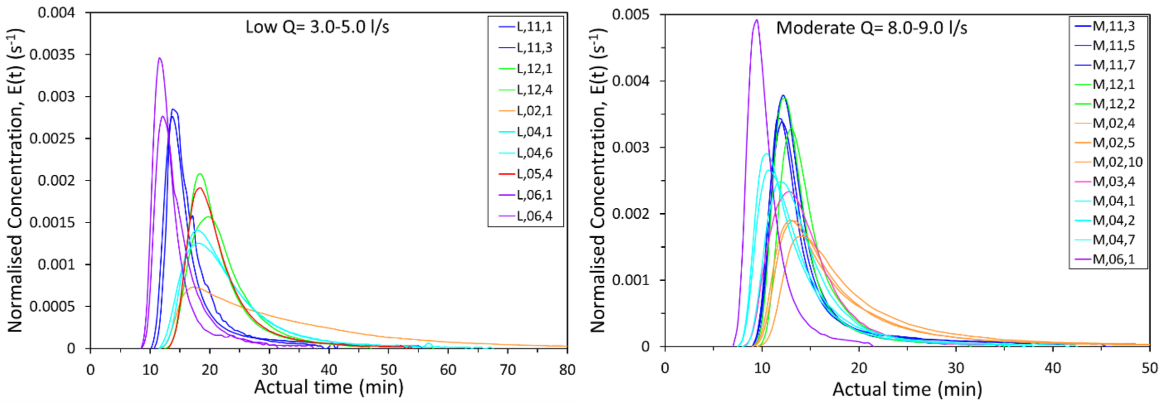

(a) Low Discharge Band, i.e. 3.0-5.0 l/s. (b) Moderate Discharge Band, i.e. 8.0-9.0 l/s.

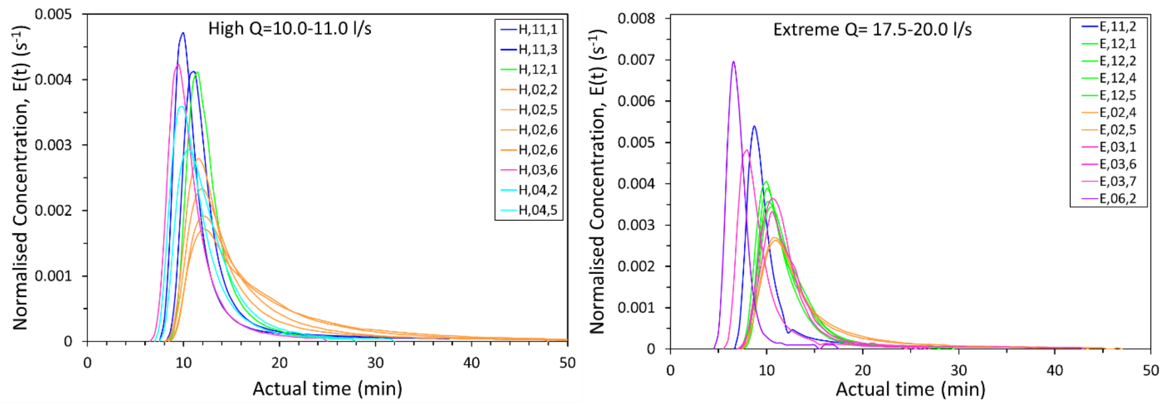

(c) High Discharge Band, i.e. 10.0-11.0 l/s. (d) Extreme Discharge Band, i.e. 17.5-20.0 l/s.

Figure 5: Different flow bands expand from Low (a) to Extreme (d), showing the seasonal plant variation effect. Concentration on y axis is normalised by the M0. RTDs demonstrated strong

affinity of late dormant season on the flow and mixing regime compared to the growth season, at all discharges. Furthermore, there is a consistent effect of discharge on the RTD shape.

The general mixing pattern shown in Figure 5 suggests that advection process dominates the flow in November and in June, while in February flow profile reaches stagnant backwater flow conditions. As a result, regardless the flow rate variation, levels of dispersion and contaminant spread are lower in June, as evidenced by the shorter tracer tails, followed by November and December; whereas greater dispersion and pollutant dilution is achieved in February. This is explained because of the smaller channel porosity induced by deflected stems, which in turn results in more obstructed flow and complexity of transit paths. Therefore, the pollutant passing through the wetland in February requires more time to be released back to the main flow, being trapped in zones of lower flow velocity, compared to the time required in June or November.

Figure 6 demonstrates the effect of discharge variation on the flow structure and on the dispersion levels, ranging between low and extreme flows. Moreover, Figure 6 embodies the effect of season, contrasting the two extremes plant stages, i.e. June (growth) and February (dormant). It is observed that larger flow rate results in lower spread and dispersion, and in shorter distribution tails. For either plant season, increase in flow rate influences the flow pattern, changing from plug flow with stagnant backwaters into plug flow. Therefore, increased flow rates contribute to more advective flow, minimising the dead zones occurrence, as explained by the shorter distribution tails.

A clear difference is distinguished in the mixing pattern between the low and high flow rate cases in Figure 6 for a fixed month. For increased flow rates, it is likely that the tracer is laterally transported further towards the edges of the wetland, resulting in some tracer capture in recirculation zones or dead zones. Holland et al (2004) investigated the hydrologic sensitivities of RTDs for various flow rates. The authors' results are in accordance with Figure 6, indicating that greater flow rates result in higher tracer concentrations and reduced spread/dispersion. The corresponding number (N) of CSTRs provides the system's mixing regime in total, if modelled as tanks in series (TIS). For the low and high flow rate cases the corresponding number of CSTRs for June is $N_{\_lowQ\text{-}June}$=14 and $N_{\_highQ\text{-}June}$=18, and for February $N_{\_lowQ\text{-}Feb}$=3 and $N_{\_highQ\text{-}Feb}$=5 respectively. This demonstrates clearly the different mixing scales in the two extreme contrasting plant seasons, where N is approximately 3 times lower in February. The possible mixing scale ranges between fully mixed flow (for N=1) and towards unmixed flow as the N tends to ∞ (N=∞ for plug flow). Both values suggest that the system has a large amount of dispersion in total. Furthermore, the fraction D_x/uL (Levenspiel, 1966) varies between 0.10 for the low flow case and 0.55 for the high flow case, further indicating in total a system that varies between large dispersion levels and backmix flow depending on the discharge.

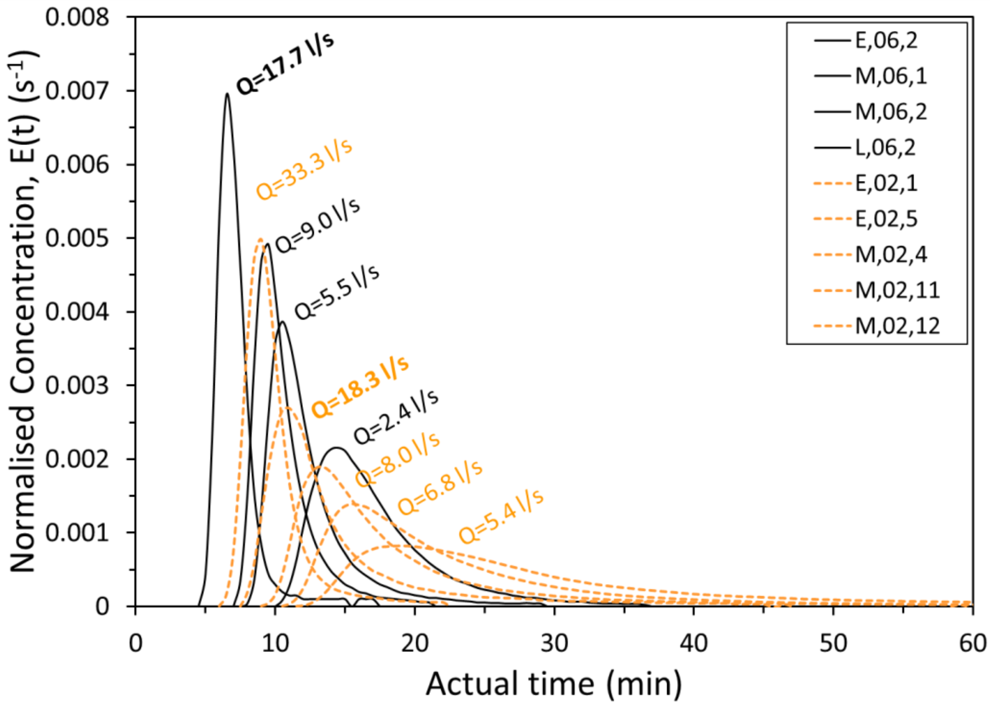

Figure 6: Effect of discharge on flow structure and dispersion between two contrasting plant ages, February (i.e. late dormant season) and June (i.e. growth season). reduction of the peak

concentration is achieved by up to three times in the late dormant season, i.e. February, compared to the growth season, i.e. June, for fixed discharge (e.g. 5.5 l/s or 18 l/s).

Variation in plant porosity between the developing and dormant seasons is a result of the variation of the stem morphology due to natural ageing and weather conditions, which overall affects both the flow pattern and the potential of reducing pollutant peak concentrations in FWS CWs. For a similar discharge, i.e. 18 l/s, in Figure 6, the mixing characteristics vary between the late dormant season (i.e. February) and the growing season (i.e. June). It is demonstrated that in the late dormant season, i.e. February, the CW may achieve reduction of the pollutant peak concentration by up to three times, compared to the growth season, i.e. June (see the relevant C_{peak} values for same flow rates – i.e. 18 l/s or 5.5 l/s – in Figure 6). A similar study by Keefe et al (2010) found that by the end of the growing seasons for their micro-climate, a distinct seasonal relation was established lodged (or flattened) vegetation characterised the solute transport in the examined wetland. However, it should be noted that although the RTDs of the present work are unimodal, this is not always the case; for example, there are studies in vegetated wetlands which observed bimodal RTDs, such as Wanko et al (2009), Musner et al (2014), and Rosqvist and Destouni (2000). It is noted that bimodal distributions reflect the preferencial paths, and potential recirculations in the system.

In summary, the prevailing flow pattern is plug flow with dead zones in all flow cases; nevertheless, the degree of dead zones is a combined effect both of flow rate, but primarily of plant season. In general, the lower flow rates resulted in more dead zones, or a greater variety of flow paths. This is explained by the fact that in laminar flow types (such as the low discharge band) diffusion is the dominant process for solute spreading, allowing more interaction and longer contact times within the system due to differential advection (see Figure 12, Left). Furthermore, during in late dormant season there are additional effects of the tracer moving through the clumps of vegetation, allowing the chemical to be trapped in the clusters of vegetation, and thus requiring longer time to be released back to the main flow at lower flow rates. However, as flow rate increases, more turbulence is generated and differential advection is reduced, which appears to outweigh the seasonal vegetation variation influence on flow profile and mixing processes.

Classification of the RTD – CRTD curves was performed for four flow rate bands (refer to Table 3.1), and parameterised by the Reynolds number, *Re*, as classified in Table 3.2. The average *Re* number for each flow rate category, namely low, moderate, high, extreme, corresponds to 2000, 3200, 4500, 7500 respectively. This identifies that the flow regime ranges between transitional and turbulent (see Table 3.2).

Table 3.2: Classification of flow regime according to flow rate.

Q (l/s)	Flow regime	Reynolds number
Q < 0.5	LAMINAR	Re < 500
0.6 < Q < 9.5	TRANSITIONAL	500 < Re < 2000
Q > 9.5	TURBULENT	Re > 2000

The dimensionless CRTD curves of the previously presented RTD curves in Figure 5 are presented in Figure 7, side by side, displaying actual time (min) on the left side, and non-dimensionlised by t_n time shown on the right side.

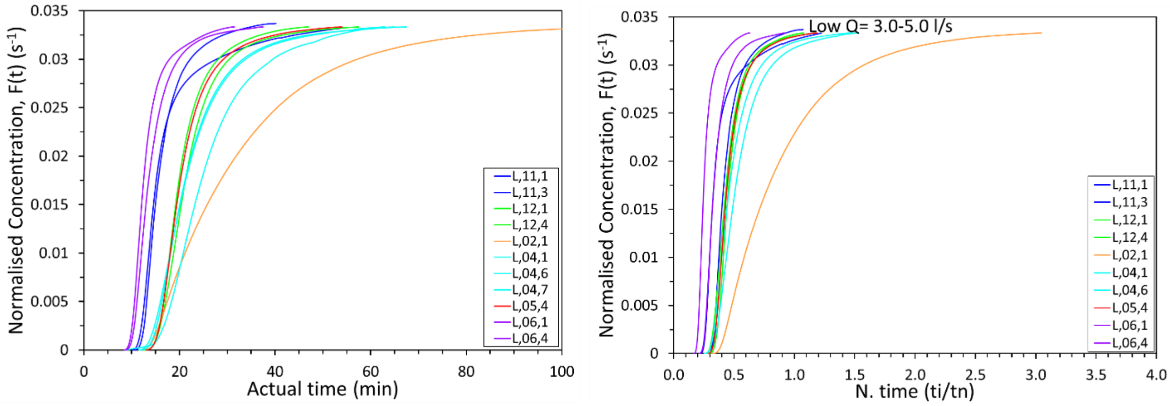

(a) Low Q = 3.0-5.0 l/s

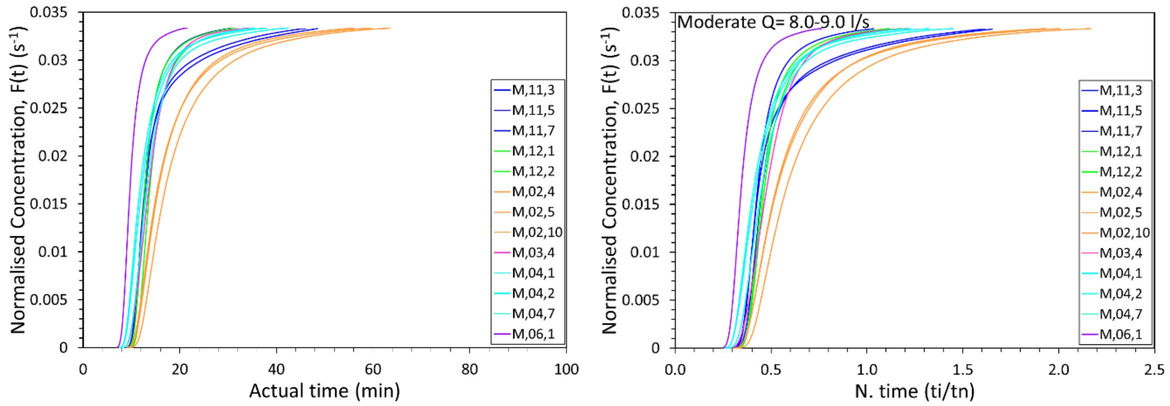

(b) Moderate Q = 8.0-9.0 l/s

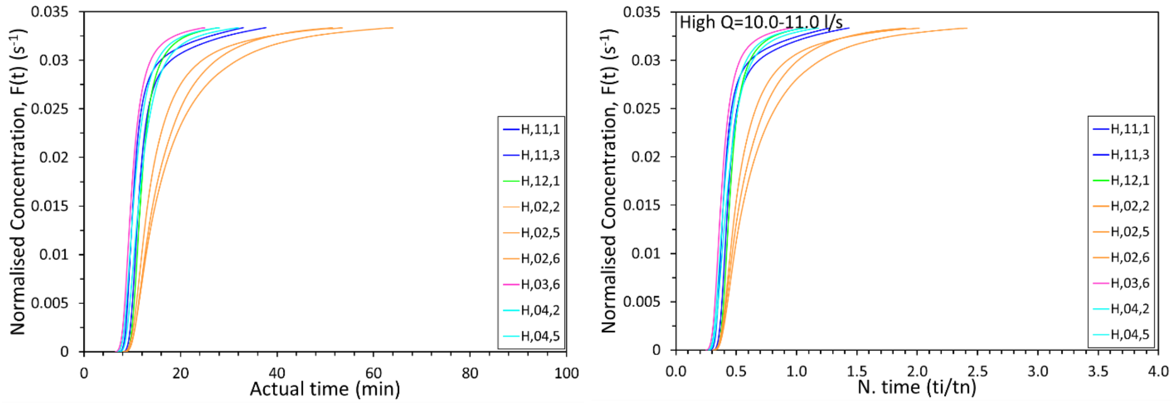

(c) High Q = 10.0-11.0 l/s

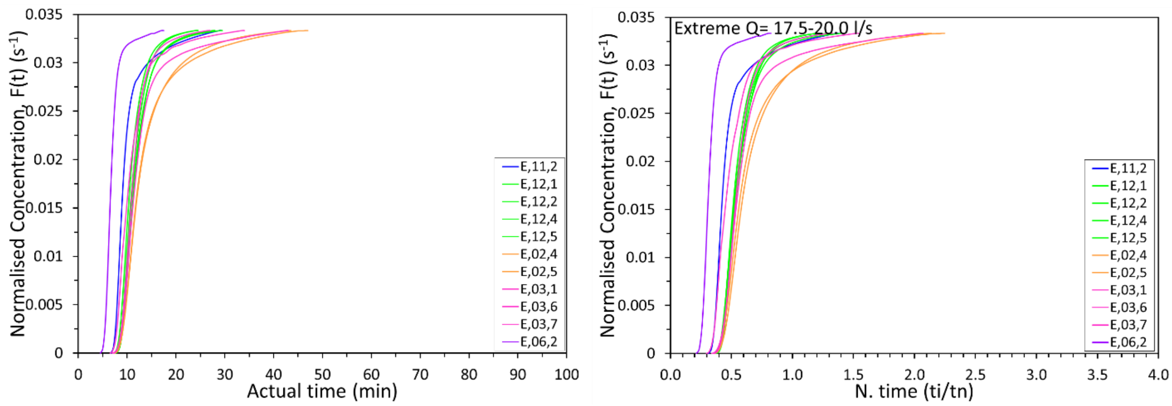

(d) Extreme Q = 17.5-20.0 l/s

Figure 7: Dimensionless CRTD curves for the different flow rate classifications, presented side by side as actual time (on the left side) and normalised time by t_n (on the right side). The flow regime follows the order from Low to Extreme. CRTD curves demonstrate a strong affinity of

plant season with HRT and mixing regime, most prevalent in the dormant season, and at low discharges. Furthermore, CRTDs demonstrate the consistent effect of discharge on mixing regime and HRT.

In left side of Figure 7 it is seen that discharge has a direct effect on the HRT, short-circuiting and mixing. As the discharge increases, CRTDs obtain gradually shorter tails and rise more steeply. Considering the seasonal effect, at normalised time, CRTD curves collapse into two main bands, i.e. February (high plant age) and the rest months, whilst June exhibits a third individual trend itself (Figure 7 right side). CRTDs in February are distinctly different, indicating large quantities of dead water in the wetland. This effect is directly associated with the clusters of deflected stems, reducing the channel porosity. At the other extreme of plant condition, i.e. June (zero stem deflection), flow pattern follows pipe flow with some longitudinal mixing, due to the larger channel porosity. Moreover, when flow rate increases, the influence of plant age is less, with all the CRTDs ranging into a narrower band; June CRTD, however, remains individual, entailing promotion of more short-circuited flows (Figure 7 right side).

Looking at the CRTDs plotted at actual time, the effect of plant season exhibits a distinct change in shape, especially ranging between the two plant age extremes (June and February). Furthermore, CRTDs show evidence of variation in mixing characteristics both due to seasonal plant variation and due to flow rate variation (left side Figure 7).

In all discharge classifications, CRTD curves suggest a system where water passes quickly through a main channel and allows for some longitudinal mixing during moderate plant ages (i.e. November – December), and during early plant ages (i.e. April, May). The mixing pattern alters notably, however, as reaching the highest plant age (i.e. February, March), suggesting plug flow with large quantities of dead zones. This result is attributed to the fully deflected stems occurring at the end of the annual plant cycle, involving nesting, resistance add-on, and creation of more pockets for mixing and dilution. Furthermore, it is noticed that regardless of the flow rate variation, CRTDs in February project invariably longer tails. The same mixing mechanism is also observed in November and March, albeit of shorter trailing edges.

On the other hand, CRTDs in December and post-March months display comparable distribution tails independently of the flow rate, while their flow pattern resembles pipe flow with some longitudinal mixing. The degree of longitudinal mixing gradually decreases, reaching mixing levels of June for all flow conditions, while advection levels (i.e. pipe flow) outweigh. This behaviour is attributed to lower stem resistance, due to the upright stem morphology during June.

The affinity of plant cycle growth with the flow resistance is described in more detail. March is the end of the annual plant cycle for the Phragmites in this UK micro-climate, and involves deflected withered stems that undergo continuous decomposition. April is the typical start of the new plant cycle; however, as there are remaining old stems, April can be described as a transition stage between the ongoing decomposition of the dead plant material, and the gradual growth of new stems. Stem population density shows gradual increase in May, as new budding stems appear. Newly grown stems are well-established in June, when wetland bed is almost clear from the recently decomposed plant material. The results of this process are directly related to the properties of the newly developed stems. Each stem resembles a bare cylinder of small diameter, while stem density per unit area is sparse; thus, none of these components promotes high vegetation drag. This explains why first arrival times shorten gradually from April to June, and why fast flow paths (short-circuiting) are essentially promoted during those months (low plant ages). The above results support the main hypothesis that seasonal plant variation influences the mixing characteristics, due to variation in stem morphology (in terms of deflection).

The CRTD curves may give an indication of the short-circuiting degree in the system, looking at the point where the steep inclination stops. As seen in Figure 7, short-circuiting increases with increase in discharge, although the flow is generally highly short-circuited even at low discharges. However, it is important to note that short-circuiting also shows a clear dependence on the plant age. At moderate and low plant ages, i.e. December, March-June respectively, the CRTDs rise steeply initially, followed by a change in their direction projecting short tails, the length of which is primarily dependent on the flow rate. At those plant ages, flow is short-circuited at values almost always greater than 0.03 (s-1) of the F(t) function. This suggests that more than 85% of the concentration mass of the tracer is short-circuited through the wetland as a straight jet, with little dispersion occurring, as inferred from the short remaining trailing edges. The most short-circuited flow occurs in June, when the CRTDs follow a steep line with a slight short tail. This advocates that in June, tracer passes by the wetland, independently of the discharge, with only minimal dispersion taking place.

It is noticeable that in February, the CRTD curves display milder incline, albeit more pronouncedly at lower flow rates. Depending on the flow rate, flow in February is short-circuited at values between 0.015 and 0.025 (s^{-1}) of the F(t) function. Therefore, it is inferred that 40% to 70% of the tracer mass passes by the wetland at low and at extreme flows respectively, whereas the remainder of the tails contribute to longitudinal mixing. Such prolonged tails suggest tracer capture in the clusters of the withered and nested stems, and evidence flow retardation, and tracer trapping in dead zones. In particular, at the low Q band (Figure 7 (a)), flow experiences a big quantity of dead zones. Nevertheless, as discharge increases, flow in the system continues experiencing stagnant backwaters, albeit of lower degree.

At normalised time, CRTDs split into two distinct groups, where most months collapse into one band, and with the extremes of plant seasons (i.e. February and June) displaying more variation. A comparison of the CRTDs among different discharges proposes that there is less dependence on flow rate compared to plant age (Figure 7 (a)–(d)). February demonstrates an apparent difference which is reflected on the mixing characteristics (i.e. stagnant regions, longer trailing edges, thus more longitudinal mixing), and on the flow properties (i.e. retardation of first arrival time, longer HRTs). As mentioned previously, June exhibits a consistent distinct mixing pattern compared to the other months.

Summarising, SW1 displays a significant variation in the mixing regime and flow pattern toward the end of dormant season, with more intense effects at low flows. Seasonal plant variation, explained through the stem deflection and morphology, alters the flow pattern from plug flow with some longitudinal mixing, into stagnant backwaters. Comparing this finding with similar or larger size systems, analogous effects should be anticipated on mixing and flow characteristics. In addition to this, HRT and reduction in C_{peak} should be expected to be much greater in CWs operating under laminar flow conditions. Overall, the corresponding effects in other wetlands might be escalated, because the majority of the controlled CW systems operate at laminar flows, and frequently at flow rates much lower than the lowest discharges of this study.

3.4 Effects of discharge and vegetation on longitudinal mixing

Figure 8 shows the variation of dispersion and discharge for the 8-month monitoring period, which despite showing some scatter, shows that in general the dispersion is independent of discharge for flow rates above 10 l/s. A relationship between D_x and Q for each month is noticed; i.e. initially a positive trend, which turns into a horizontal trend beyond for flow rates above 10 l/s. It is noticeable that this limit varies with month. This is attributed to the resistance of stems on the flow; in particular, in low flow velocity, internal hydraulics are vegetation dominated, whilst in high flow velocities, internal hydraulics are flow dominated. As flow rate increases, the effect of bed boundary and differential advection seems to be less significant, resulting in lower longitudinal dispersion. The monthly trend of the mean monthly longitudinal dispersion coefficient, D_x, is shown in Figure 9, the results indicate that this dispersion is higher between November to February, and gradually reduces from March to June, which is consistent with the annual plant cycle growth. December was a particularly wet month, hence the dispersion values in December are indicated by grey circle colour in the same figure; and have been omittem from the general trend, indicated by the dashed line.

In order to explain the results, recall of the plant cycle and natural ageing processes is required, i.e. November experiences stem foliage drop, which might create clusters of mixed foliage travelling in the wetland. In this case, the tracer may encounter some dead regions, as demonstrated by the relatively long trailing edges in Figure 5 and Figure 7. The large D_x values obtained in February are attributed to the dead zones promoted due to the clusters of the deflected stems (i.e. reduced channel porosity). Furthermore, large D_x values in February result from the long trailing edges of the RTDs, which are reported to increase the D_x (Rutherford, 1994).

March D_x values present a wider scatter compared to other months, albeit they follow an overall mild inclination, and they stay generally lower than February D_x values. However, the ongoing decomposition of deflected stems occuring in March (as the last month of the annual plant cycle), as well as other random natural factors, including wind action which promotes deposition of the total or parts of the reed stems, and stem debris deposition, may drastically contribute to the variation in the D_x levels, altering the local flow paths and dead water areas.

With the start of the new plant cycle, low plant ages, i.e. April, May and June, display overall lower D_x values. Nevertheless, April experiences higher D_x coefficients compared to June, as a result of the fraction of the remaining stems, ongoing decomposition. As time passes though, decomposition of remaining old stems is completed, and thus the stem population density reduces and the channel porosity increases. Such decrease in D_x is sensible and is reported by Nepf et al (1997), who observed a reduction of D_x with stem population density.

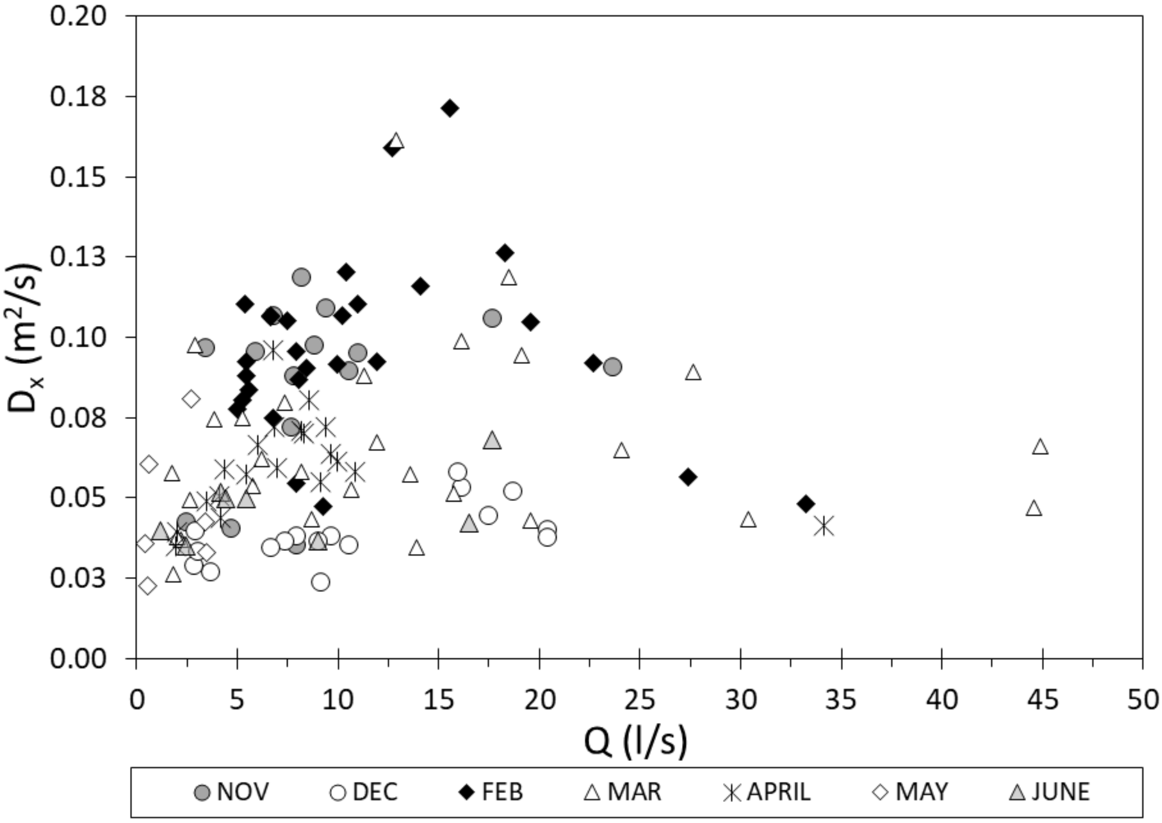

Figure 8: Relationship between longitudinal dispersion coefficient, D_x, and flow rate, Q, including the best fit line. D_x is classified as per month.

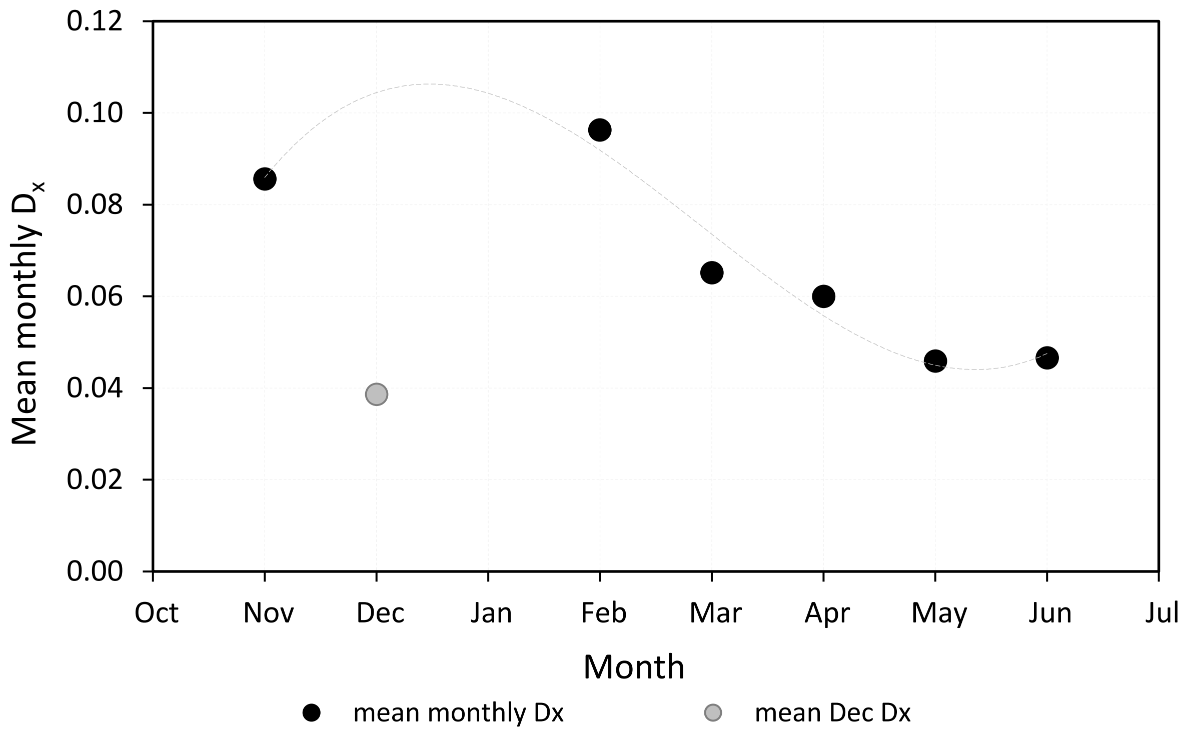

Figure 9: Mean monthly D_x is plotted against month to show the average monthly trend in longitudinal dispersion coefficient. Dispersion values in December are indicated by grey circle colour, and have been omittem from the general trend, indicated by the dashed line, as December was a particular wet month.

One study that investigated the longitudinal dispersion and used planted emergent Phragmites in a laboratory flume found slight reduction of the longitudinal mixing coefficient with flow depth and with discharge (Shucksmith, 2008). The magnitude of D_x coefficients in SW1 is comparable, although slightly greater than Shucksmith's (2008) D_x coefficients (i.e. 0.005-0.018 m2/s), who conducted tests in reeds and in similar discharges (i.e. 10-30 l/s) for two contrasting plant seasons, albeit in laboratory conditions (entailing different plant decay, and size of the systems (full-scale and pilot-scale)). The current study was conducted in outdoor conditions, under a typical UK micro-climate, while Shucksmith's (2008) observations/tests were conducted in the laboratory, where the air temperature must have been favourable for the plants to develop fully unitl week 50. Limitations of the current study includes the fact that the typical British summer is relatively dry, hence decreasing the water tables, causing no dry weather flow rates to be registered by the end of June. As a consequence, there is a paucity of data for three to four months, between July and October, when Phragmites reach their highest heights and development. However, stem diameter observations did not show any signinticant change in the stem diameters annually, that could play role in the channel porosity (or canopy frontal area) variation. Likewise, the fact that no more plants growth happens between those months, suggests that stem packing density stays fixed during those months. Therefore, it could be assumed that similar trends as June would occur in the mixing regime and the HRT until September, given that there is no change in the stem density and no decay occurs to affect the plant morphology or block the flow depth.

A notable difference in the dispersion values, D_x between this study and Nepf et al (1997) was observed, where D_x coefficients obtained in this study were 10^2 to 10^3 times larger than Nepf et al's (1997) D_x coefficients. In both studies stem population densities and stem diameters are similar, however the length (L) to width (W) ratio (aspect ratio) in the laboratory study by Nepf et al (1997) was 20/0.38 = 52.6, whereas the aspect ratio of the current study is 5 to 13 times larger. The difference in the width between the two systems is large, consequently resulting in substantially different system aspect ratios, with the associated field effects. According to Persson (2000), the aspect ratio affects significantly the amount of mixing. In particular, high aspect ratios promote plug flow, hence diminish dispersion, and therefore the large difference in the dispersion coefficients is possibly attributed to the aspect ratio of each system. In addition to this, the random nature of the presented CW, including potential hyporheic exchange between the bed and the water column, might also have played a role in the divergence of the D_x values obtained between the two studies. Another study providing experimental data on D_x including Phragmites is conducted by Shucksmith (2008). The author used real Phragmites in a flume with aspect ratio of 14.5/1.22 = 11.9, and for testing discharges between 10 to 30 l/s – similar to the current study – the range of D_x obtained was between 0.004 and 0.018 m^2/s, which is 10^2 times smaller than the current study's D_x results. Besides the fact that higher aspect ratio decreases the D_x, which is likewise the case for Shucksmith's (2008) results, it has to be noted that both laboratory studies discussed were conducted under ideal rectangular channel shapes/geometry – which might promote boundary shear due to the narrow dimension and hence internal mixing coefficient – and under zero wind interference. In addition to this, experimental data obtained by Ioannidou & Pearson (2018) demonstrated that the width of the treatment unit is a more relevant dimension to the solute/contaminant mixing characteristics compared to the depth. This finding indicates that width is a more important dimension compared to depth in affecting mixing characteristics in different scale systems.

3.5 Hydraulic parameters (effect of vegetation and Q on HRT, on λ and on S_m)

Figure 10 illustrates the mean residence time, t_m, (which corresponds to the actual measured residence time of each tracer test) against flow rate. On the same plot, the theoretical (or nominal) residence time curve, t_n, is presented accounting for the plant porosity during the developing season i.e. for upright stems (see section 2.2): for η_g=0.995 presented by the dashed line; recall that theoretical residence time curve approximates the porosity from May to October. It is observed that the upright stem conditions, albeit incorporated in the volume calculation, has a negligible impact on the channel porosity. Results suggest that seasonal plant variation affects the HRT and the short-circuiting. Results advocate that there is notable short-circuiting in the system, which is further quantified and confirmed by the short-circuiting index, S_m, as registered in Table 3.1. Figure 10 shows that the larger the deviation from the measured values, t_m, to the theoretical time curve, t_n, the shorter the tracer stays in the CW, which indicates that the tracer follows the fast flow paths. In addition to this, late plant dormant stages (i.e. February, March) result in larger HRTs, compared to developing plant stages (i.e. November, June). Stem resistance in the wetland increases with the deflection of plants as a result of their ageing. Furthermore, it is observed that short-circuiting is greater in the growth season (i.e. November, June).

Overall, this CW displays lower short-circuiting at lower discharges. As an unbunded system by construction, water is shallow and flows through swiftly, promoting high short-circtuiting levels. Interestingly, the newly developed plant season appears to create greater short-circuiting, as observed in the results for June (Figure 10).

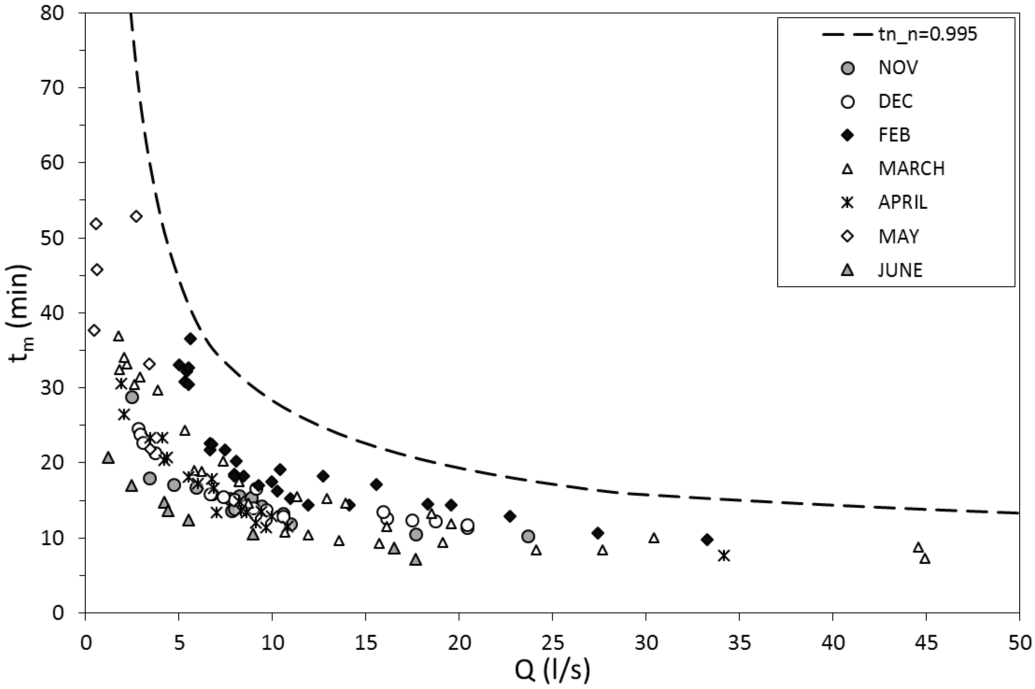

Figure 10: Relationship between mean residence time, t_m, nominal residence time, t_n, and flow rate, Q.

The hydraulic efficiency, λ, of the CW lays between the satisfactory quality and the good quality band, according to Persson et al’s (1999) classification standards (Table 2.2). In general, λ does not drop below 0.5, which initially and apparently indicates that the system functions satisfactorily and in most cases very well, in terms of mixing and active water volume utilisation. However, there is a contradiction between the relatively high-short-circuiting levels and the good hydraulic efficiency. The effective volume ratio, *e*, ranges from low (i.e. 0.4) to highly satisfactory (i.e. 0.8), indicating an affinity with the plant season, particularly between June and February. Furthermore, if plant ageing were not taken into consideration, one would deduce that λ increases with discharge in this CW. However, in effect, it is observed that λ is affected by the plant stage, displaying lowest values in February including the majority of the satisfactory λ values. March receives a sporadic, wide spread attributed to the aforementioned discussion. December and June operate very well with the highest λ values regardless the discharge. In contrast to these results, Holland et al (2004) found minimal effect of the discharge on λ, but that was attributed to the limitation in the discharges tested, between 1.2 and 3.2 l/s, which belong to the laminar flow regime in terms of *Re*, and may not be typical of natural flow rates.

Overall, it is observed that λ has an inverse relationship with D_x; therefore, higher λ values are observed for lower longitudinal mixing cases. However, some degree of mixing is essential to attenuate pollutant concentration in wetlands. This indicates remediation actions in the CW to increase the HRT, because various agricultural runoff pollutants cannot be treated in the order of hours, but require days.

A relationship of the short-circuiting index S_m used in this study against flow rate is presented in Figure 11. The way that S_m is defined designates that values closer to 1 involve higher short-circuiting. There appears to be two different curves fitting the dataset, as shown in Figure 12; namely, a linear upper bound trend followed in November, December, partly in May, and June, when the stems are predominantly vertical. There is also a lower bound curved trendline, representing the decay plant period in February and partly in March, when the stems are decayed. The tracer tests in April and May, lay in-between those conditions, probably because the new grown stems are still developing and keep changing the internal hydraulics, until they establish well in June. Although there is a paucity of data between July and

September, it is regarded that the short-circuit will follow the linear trendline, because of the non-changing, upright stem morphology.

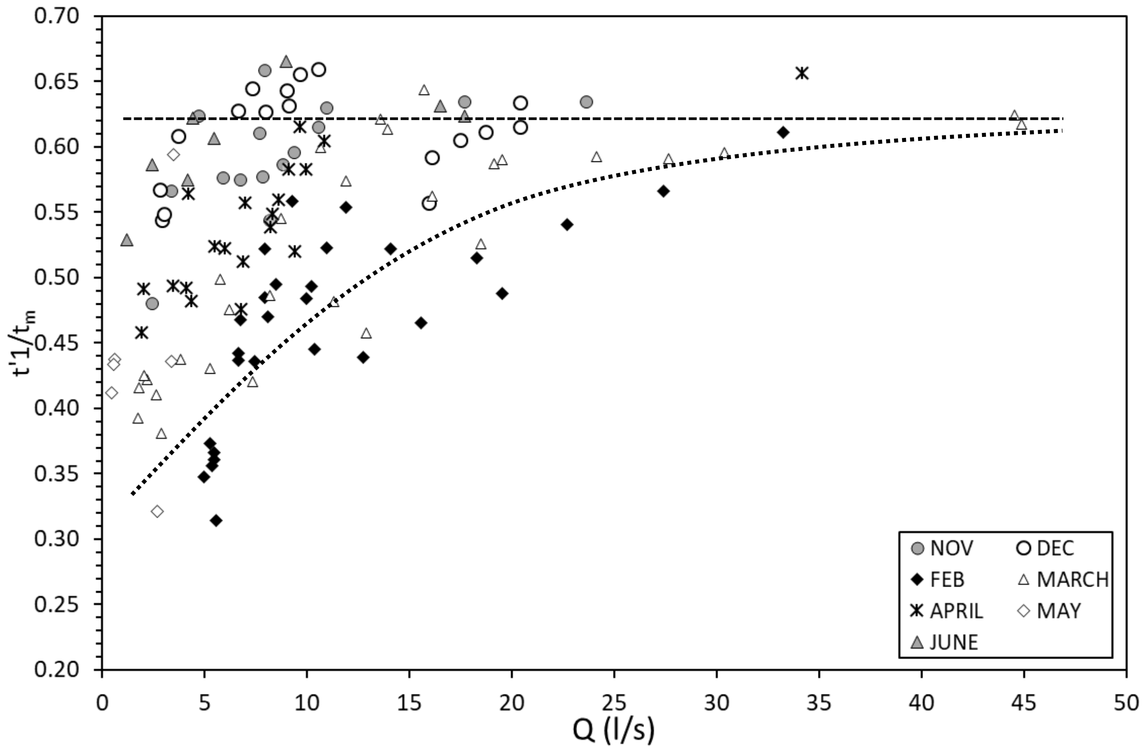

Figure 11: Relationship between short-circuiting index, S_m, and flow rate, Q. The upper dashed line approximately represents the November and June data, and the dotted line lower bound limit represents the February data.

Overall, S_m results suggest that on average there is significant amount of short-circuiting in the wetland with several cases of higher index incidents. It is observed that lower flow rates result in slightly lower short-circuiting index. However, interestingly, S_m is more influenced by the plant age rather than by the flow rate. Figure 11 shows that S_m is significantly lower in February, when plants are bent over, compared to December and June, when stems are upright. However, as noted perviously, this does not entail the similar trends for hydraulic efficiency.

To elucidate the mixing within the CW, tracer measurements were conducted on one cross-section of the CW under two contrasting discharges in February, using four Cyclops-7 probes along the wetland cross-section. The two internal mixing studies for different discharges, low, Q_{low} = 10 l/s, and high, Q_{high} = 38 l/s, are illustrated in Figure 12. The transverse locations of the probes are illustrated and labelled on the plan map of the CW in Figure 1. In the low discharge case (Figure 12, Left), the areas under each curve (M_0) are similar ($M_{0\_1,2,3} \cong 1.9 \cdot 10^6$), except for the location 4 ($M_{0\_4} \cong 1.6 \cdot 10^6$). Noticeable change in concentration mass is marked. Differential advection is overt, as tracer travels faster through at the centreline (locations 2 and 3) (see Figure 12, Left), while at location 1 the mean residence time needs approximately 1 hour for the tracer to pass through; namely essentially doubled t_m compared to the middle of the cross-section. All RTDs are unimodal, with the typical skewed bell-shape, apart from location 1, which is bimodal. This is a sign of recirculated or trapped tracer in that side of the system. In the high discharge case (Figure 12, Right), HRTs are 10 times shorter transversely compared to the low discharge case (from 6 to 11 min). For this case, location 1 has 50% lower area under the curve ($M_{0\_1} \cong 1.6 \cdot 10^5$) compared to the other three locations ($M_{0\_2,3,4} \cong 3.5 \cdot 10^5$). It can be seen that the increase in Q fosters flow shear velocity, with more differential advection occurring closer to the channel boundaries. The low Q case suggests almost plug flow conditions, whilst in greater flows a preferential path is prevalent through location 3. The concentration levels are elevated, but tracer curves keep the same general trends as in the low discharge case. This could be explained as that in the higher discharges, the increase in water level across the cross-section allows for faster water movement also towards the banks. This is reflected by the closer HRTs values between the four monitoring locations at the high discharge case, which are 6-7 min in the middle and 10-11 min towards the edges. It is inferred that lower discharges promotes an increase in the number of flow paths and dead-zones, resulting in increased differential advection, reflected in the measured tracer residence times.

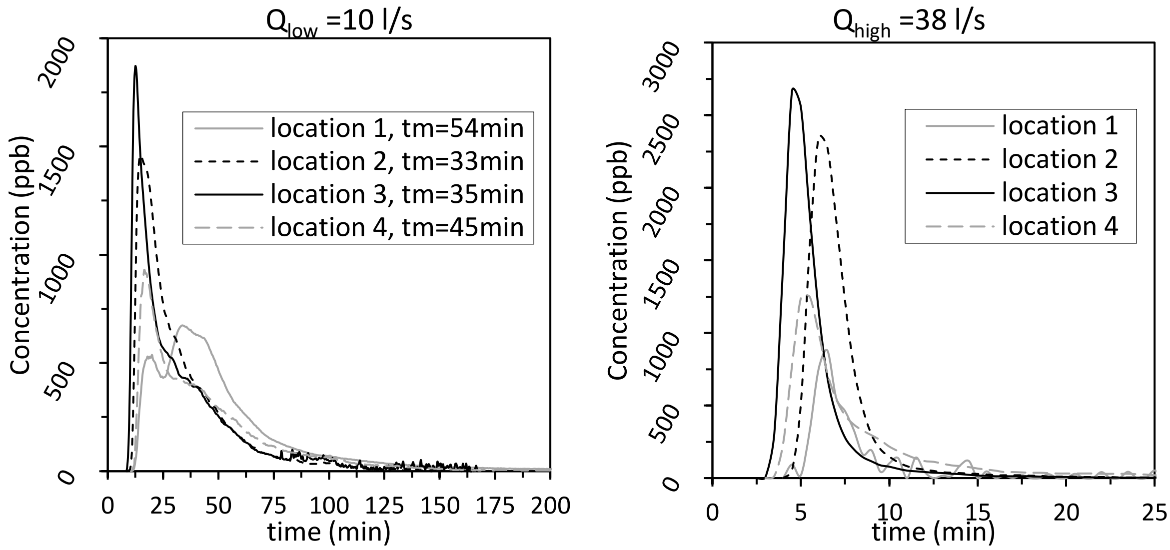

Figure 12: Internal mixing study on one cross-section of the CW under two contrasting flow rates, low (Left) and high (Right).

4. CONCLUSIONS

This study reports field tracer data collected in a full-scale constructed wetland, and relevant Residence Time Distribution (RTD) hydrodynamic parameters for different flow rates, over a monitoring period of eight months under the presence of natural vegetation. The results demonstrated that, as expected, higher flow rates resulted in higher advection levels and shorter hydraulic residence times (HRTs), but flow rate variations had a small effect on the shape of the RTD curves. Vegetation ageing as a natural process in the CW, demonstrated greater influence on the mixing regime and characteristics compared to flow rate variation, particularly at the end of dormant season (February and March). Dimensionless Cumulative Residence Time Distribution (CRTDs) curves suggest that the longitudinal dispersion coefficient varies significantly between the growth and the wither vegetation periods, indicated by the RTD trailing edges. The longitudinal dispersion initially increased with flow rate, however, beyond a discharge of around 10 l/s, the longitudinal dispersion becomes independent of discharge; it is also noticeable that, longitudinal dispersion is significantly dependent on the vegetation characteristics.

The results suggest that the plant ageing factor has to be taken into consideration in the study of wetland hydrodynamics, in the design and maintenance of CWs, and it has to be appropriately incorporated in the modelling tools, as it influences the mixing regime and involved hydraulic parameters (HRT, hydraulic efficiency). As the flow rate range of this study was conducted between transitional and turbulent flow regimes, and given that the transitional flow regime evidenced the greatest influence by the plant ageing, it is inferred that plant ageing has potentially a high impact on laminar flow regimes, in which the majority of the CWs operate, and is recommended to be accounted for.

ACKNOWLEDGEMENTS

The work has been financially supported by the School of Engineering, University of Warwick, through a PhD scholarship for V. Ioannidou, and was also partially supported by the Natural Environment Research Council [grant number NE/R003645/1]. The authors gratefully acknowledge the RSPB Hope Farm members' support and permission to access their wetlands, technical support from Ian Baylis in the School of Engineering, and access to raingauge data from Andre Ramos from Cranfield University. We thank the editor and three anonymous reviewers for their constructive comments, which helped us to improve the manuscript.

REFERENCES

Agunwamba, J.C. (2006). Effect of the location of the inlet and outlet structures on short-circuiting: Experimental investigation. *Water environment research*, 78(6), 580-589.

Bodin, H., Mietto, A., Ehde, P.M., Persson, J. & Weisner, S.E.B. (2012). Tracer behaviour and analysis of hydraulics in experimental free water surface wetlands. *Ecological Engineering*, 49, 201-211.

BS 3680-2A: 1995; ISO 9555-1: 1994. Measurement of liquid flow in open channels. Dilution methods. General.

BS 3680-4A: 1981. Methods of measurement of liquid flow in open channels. Weirs and flumes. Method using thin-plate weirs.

Burke, E. N., & Wadzuk, B. M. (2009). The effect of field conditions on low Reynolds number flow in a wetland. *Water research*, 43(2), 508-514.

Chyan, J. M., Tan, F. J., Chen, I. M., Lin, C. J., Senoro, D. B., & Luna, M. P. C. (2014). Effects of porosity on flow of free water surface constructed wetland in a physical model. *Desalination and Water Treatment*, 52(4-6), 1077-1085.

Danckwerts, P.V. (1953). Continuous flow systems: Distribution of residence times. Chemical Engineering Science, 2(1), 1-13.

German, J., Jansons, K., Svensson, G., Karlsson, D., & Gustafsson, L. G. (2005). Modelling of different measures for improving removal in a stormwater pond. *Water science and technology*, 52(5), 105-112.

Ghisalberti, M., & Nepf, H. (2005). Mass transport in vegetated shear flows. *Environmental fluid mechanics*, 5(6), 527-551.

Holland, J.F., Martin, J.F., Granata, T., Bouchard, V., Quigley, M. & Brown, L. (2004). Effects of wetland depth and flow on residence time distribution characteristics. *Ecological Engineering*, 23, 189-203.

IAPWS, 2008. The International Association for the Properties of Water and Steam. http://www.iapws.org/. [date accessed: 01/06/2016]

Ioannidou, V.G. & Pearson, J.M. (2018). Hydraulic & Design Parameters in Full-Scale Constructed Wetland & Treatment Units: Six Case Studies. *Environmental Processes*. DOI: 10.1007/s40710-018-0313-8.

Jenkins, G. A., & Greenway, M. (2005). The hydraulic efficiency of fringing versus banded vegetation in constructed wetlands. *Ecological Engineering*, 25(1), 61-72.

Kadlec, R. H. (1990). Overland flow in wetlands: vegetation resistance. *Journal of Hydraulic Engineering*, 116(5), 691-706.

Kadlec, R.H. (1994). Detention and mixing in free water wetlands. *Ecological Engineering*, 3, 345-380.

Kadlec, R.H. (2009). Comparison of free water and horizontal subsurface treatment wetlands. *Ecological Engineering*, 35, 159-174.

Kadlec, R.H. & Wallace, S.D., 2009. Treatment wetlands, 2nd ed. CRC Press, Boca Raton, FL.

Keefe, S. H., J. S. (Thullen) Daniels, R. L. Runkel, R. D. Wass, E. A. Stiles, and L. B. Barber (2010), Influence of hummocks and emergent vegetation on hydraulic performance in a surface flow wastewater treatment wetland, Water Resour. Res., 46, W11518, doi:10.1029/2010WR009512.

Koskiaho, J. (2003). Flow velocity retardation and sediment retention in two constructed wetland-ponds. *Ecological Engineering*, 19, 325-337.

Kröger, R., Moore, M.T., Locke, M.A., Cullum, R.F., Steinriede, R.W., Testa, S., Bryant, C.T., & Cooper, C.M. (2009). Evaluating the influence of wetland vegetation on chemical residence time in Mississippi Delta drainage ditches, *Agricultural Water Management*, 96(7), 1175-1179. ISSN 0378-3774, https://doi.org/10.1016/j.agwat.2009.03.002.

Lightbody, A. F. & Nepf, H. M. (2006). Prediction of velocity profiles and longitudinal dispersion in emergent salt marsh vegetation. *Limnology and Oceanography*, 51(1), 218-228.

Min, J. H. & Wise, R. W., (2009). Simulating short-circuiting flow in a constructed wetland: the implications of bathymetry and vegetation effects. *Hydrological Processes*, 23, 830-841.

Nepf, H. M., Mugnier, C. G., & Zavistoski, R. A. (1997). The effects of vegetation on longitudinal dispersion. *Estuarine, Coastal and Shelf Science*, 44(6), 675-684.

Nepf, H.M. (1999). Drag, turbulence, and diffusion in flow through emergent vegetation. *Water Resources Research*, 35(2), 479-489.

Nepf, H. M. (2012 a). Hydrodynamics of vegetated channels. *Journal of Hydraulic Research*, 50(3), 262-279.

Nepf, H.M. (2012 b). Flow and transport in regions with aquatic vegetation. *Annual Review of Fluid Mechanics*, 44, 123-142.

Nepf, H., Ghisalberti, M., White, B., & Murphy, E. (2007). Retention time and dispersion associated with submerged aquatic canopies. *Water Resources Research*, 43(4).

Okamoto, T. A., Nezu, I., & Ikeda, H. (2012). Vertical mass and momentum transport in open-channel flows with submerged vegetations. *Journal of Hydro-environment Research*, 6(4), 287-297.

Persson, J., Somes, N.L.G. & Wong, T.H.F. (1999). Hydraulics efficiency of constructed wetlands and ponds. Water Science and Technology, 40(3), 291-300.

Persson, J. (2000). The hydraulic performance of ponds of various layouts.*Urban Water*, 2(3), 243-250.

Robert, A. (2003) “River Processes: A Introduction to Fluvial Hydraulics.” Arnold.

Sabokrouhiyeh, N., Bottacin-Busolin, A., Savickis, J., Nepf, H., & Marion, A. (2017). A numerical study of the effect of wetland shape and inlet-outlet configuration on wetland performance, *Ecological Engineering*, 105, 170-179. ISSN 0925-8574, https://doi.org/10.1016/j.ecoleng.2017.04.062.

Shih, S.F. & Rahi, G.S. (1982). Seasonal variations of Manning’s foughness coefficient in a subtropical marsh. Transactions of the American Society of Agricultural Engineers, 25(1), 116-120.

Shucksmith, J. D. (2008). Impact of vegetation in open channels on flow resistance and solute mixing (Doctoral dissertation, Sheffield).

Somes, N.L.G., Persson, J. & Wong, T.H.F. (1998). Influence of Wetland Design Parameters on the Hydrodynamics of Stormwater Wetlands. *Hydrastorm*, Adelaide, 27-30 September, 1998, 123-128.

Su, T. M., Yang, S. C., Shih, S. S., & Lee, H. Y. (2009). Optimal design for hydraulic efficiency performance of free-water-surface constructed wetlands. *Ecological Engineering*, 35(8), 1200-1207.

Taylor, G. (1953). Dispersion of soluble matter in solvent flowing slowly through a tube. Proceedings of the Royal Society A, 219, 186-203.

Thackston, E.L., Shields, D. & Schroeder, P.R. (1987). Residence time distributions of shallow basins. *Journal of Environmental Engineering*, 113(6), 1319-1332.

Weisner, S. E., & Thiere, G. (2010). Effects of vegetation state on biodiversity and nitrogen retention in created wetlands: a test of the biodiversity–ecosystem functioning hypothesis. *Freshwater Biology*, 55(2), 387-396.

Werner, T.M. & Kadlec, R.H. (2000). Wetland residence time distribution modelling. *Ecological Engineering*, 15, 77-90.

Wörman, A., & Kronnäs, V. (2005). Effect of pond shape and vegetation heterogeneity on flow and treatment performance of constructed wetlands, *Journal of Hydrology*, Volume 301 (1-4), 123-138. ISSN 0022-1694, https://doi.org/10.1016/j.jhydrol.2004.06.038.